On the Flow Problem in Water Distribution Networks: Uniqueness and Solvers

Manish K. Singh and Vassilis Kekatos, *Senior Member, IEEE*

Abstract—Increasing concerns on the security and quality of water distribution systems (WDS), along with their role as smart city components, call for computational tools with performance guarantees. To this end, this work revisits the physical laws governing water flow and provides a hierarchy of solvers having complementary value. Given water injections in a WDS, finding the corresponding water flows within pipes and pumps together with the pressures at all nodes constitutes the water flow (WF) problem. The latter entails solving a set of (non)-linear equations. It is shown that the WF problem admits a unique solution even in networks hosting pumps. For networks without pumps, the WF solution can be recovered as the minimizer of a convex energy function. The latter approach is extended to networks with pumps but not in cycles, through a stitching algorithm. For networks with non-overlapping cycles, a provably exact convex relaxation of the pressure drop equations yields a mixed-integer quadratic program (MIQP)-based WF solver. A hybrid scheme combining the MIQP with the stitching algorithm can handle water networks with overlapping cycles, but without pumps on them. Each solver is guaranteed to converge regardless initialization. Two of the solvers are numerically validated on a benchmark WDS.

Index Terms—Water flow equations, convex relaxation, graph reduction, mixed-integer quadratic program, second-order cone constraints, uniqueness.

I. INTRODUCTION

Water distribution systems serve as a critical infrastructure across the world. The direct dependence of human lives on the availability of water has motivated research on the security, resiliency, and quality of water supply systems [1], [2], [3]. The high cost of installation for different WDS components renders long-term network planning an important problem [4], [5]. Furthermore, the relatively expensive operation of a WDS is primarily attributed to the electricity cost for running pumps to properly circulate water [6], [7]. Thus, optimal pump scheduling for the daily operation of a WDS is a pertinent research problem [8], [9]. An inevitable component of the aforementioned computational problems is satisfying the physical laws governing water flow. Mathematically, the *water flow (WF) equations* consist of a set of linear equations ensuring mass conservation, along with a set of non-linear equations arising from energy and momentum conservation [10].

Solving the WF equations constitutes the *water flow problem*. Specifically, given water demand at all nodes, the standard WF task aims at finding the water flows within all pipes and the pressures at all nodes complying with the

M. K. Singh and V. Kekatos are with the Bradley Dept. of Electrical and Computer Engineering, Virginia Tech, Blacksburg, VA 24061, USA. Emails: {manishks,kekatos}@vt.edu. This work was supported by the U.S. National Science Foundation under Grant 1711587.

WF equations. Modern renditions of the WF problem may incorporate pumps, valves, and pressure-based demands [11], [12]. Either way, handling the non-linear equations stemming from the conservation of energy and momentum remain the core challenge [10].

Existing WF solvers update iteratively a set of WF variables, which could be the pipe flows, the loop flows, the nodal pressures, or combinations thereof [13]. These solvers can be broadly classified into those relying on successive linear approximations, and those relying on Newton-Raphson-type of updates [10]. For example, the WF solver of [14] constitutes a fixed-point iteration and belong to the former class, while EPANET (perhaps the most widely used WF solver) belongs to the latter class [12]. In fact, most of the schemes within each class have been shown to be equivalent to each other upon a (non)-linear transformation of variables [13], [10]. To reduce the problem dimensionality, different preprocessing, partitioning, and reformulations have been reported [15],[16],[17].

The aforesaid solvers exhibit two major shortcomings. First, their convergence and rate of convergence depend critically on initialization. For example, it has been numerically demonstrated that EPANET fails to find a WF solution for some practical water networks [18], [19]. Nonetheless, proper initialization may be challenging when dealing with stochastic planning or risk analysis, where the WF task has to be solved repeatedly and under varying demands [16]. As a second shortcoming, the existing solvers do not naturally extend to optimal water flow (OWF) formulations. Therefore, most OWF efforts resort to linear approximations; non-linear local optimization; or slow zero-order algorithms building on an independent WF solver such as EPANET; see [1]. Such OWF approaches lack scalability and/or optimality guarantees.

The contribution of this work is in two fronts. After a brief modeling of water networks (Section II), this work first establishes that given the water injections at all nodes, there exists a *unique* set of water flows and nodal pressures satisfying the (non)-linear WF equations (Section III). Second, it puts forth a suite of solvers that can provably recover the WF solution under different water network setups; see also the flowchart of Fig. 1:

i) In networks without pumps, the WF solution can be recovered as the minimizer of a convex problem. The problem minimizes a judiciously selected energy function under a constrained (Section IV-A) or unconstrained formulation (Section IV-B).

ii) This energy function-based approach is then extended to networks where pumps do not lie on cycles through the *stitching algorithm* of Section IV-C.

iii) In networks with no overlapping cycles, the MIQP scheme of Section V can find the WF solution.

iv) A hybrid procedure combining the stitching algorithm and the MIQP solver handles networks having overlapping cycles, but without pumps on them (Section VI).

These novel solvers not only operate under different network configurations, but constitute a hierarchy: Solver *ii)* builds on *i)*; and solver *iv)* builds on *ii)* and *iii)*. Numerical tests on a benchmark network evaluate the correctness and running times for *i)* and *iii)*; and compare them against the EPANET solver (Section VII).

Regarding notation, lower- (upper-) case boldface letters denote column vectors (matrices). Calligraphic symbols are reserved for sets. The vectors of all zeros, all ones, and the n-th canonical vector are denoted respectively by $\mathbf{0}$, $\mathbf{1}$, and $\mathbf{e}_n$, while their dimension will be clear from the context. The symbol $^\top$ stands for transposition.

II. WATER DISTRIBUTION SYSTEM MODELING

A WDS can be represented by a directed graph $\mathcal{G} := (\mathcal{N}, \mathcal{P})$. Its nodes are indexed by $n \in \mathcal{N} := \{1, \ldots, N\}$ and correspond to water reservoirs, tanks, and points of water demand. Let d_n be the rate of water injected into the WDS from node n. For reservoirs apparently $d_n \geq 0$; for nodes with water consumers $d_n \leq 0$; tanks may be filling or emptying; and $d_n = 0$ for junction nodes.

The edges in set $\mathcal{P}$ with cardinality $P := |\mathcal{P}|$, are associated with pipes and pumps. The directed edge $p = (m, n) \in \mathcal{P}$ models the water pipe between nodes m and n. Its water flow is denoted by f_{mn} or f_p depending on the context. If water flows from node m to n, then $f_{mn} \geq 0$; otherwise $f_{mn} < 0$.

Conservation of water flow dictates that for all $n \in \mathcal{N}$

$$d_n = \sum_{k:(n,k)\in\mathcal{P}} f_{nk} - \sum_{k:(k,n)\in\mathcal{P}} f_{kn}.$$

The connectivity of the WDS is captured by the edge-node incidence matrix $\mathbf{A} \in \mathbb{R}^{P \times N}$ with entries

$$A_{p,k} = \begin{cases} +1, & k = m \\ -1, & k = n \\ 0, & \text{otherwise} \end{cases} \quad \forall \, p = (m, n) \in \mathcal{P}. \quad (1)$$

Given $\mathbf{A}$ and upon stacking flows and injections respectively in $\mathbf{f} \in \mathbb{R}^P$ and $\mathbf{d} \in \mathbb{R}^N$, the conservation of water flow across the WDS can be compactly expressed as

$$\mathbf{A}^\top \mathbf{f} = \mathbf{d}. \quad (2)$$

The operation of WDS is also governed by pressures. Water pressure is surrogated by *pressure head*, defined as the equivalent height of a water column in meters, which exerts the surrogated pressure at its bottom. The pressure head (henceforth *pressure*) at node n is denoted by h_n. The pressures at all WDS are referred to a common geographical elevation. Moreover, the pressure h_r at a reservoir node $r \in \mathcal{N}$ typically serves as the pressure of reference.

With water flowing in a pipe, pressure drops along the direction of flow due to friction. The pressure drop across pipe $(m, n) \in \mathcal{P}$ is described by the Darcy-Weisbach law [20]

$$h_m - h_n = c_{mn} \text{sign}(f_{mn}) f_{mn}^2 \quad (3)$$

where the constant c_{mn} depends on pipe dimensions [9], and the sign function is defined as

$$\text{sign}(x) := \begin{cases} +1, & x > 0 \\ 0, & x = 0 \\ -1, & x < 0 \end{cases}.$$

The pressures at all nodes are collected in vector $\mathbf{h} \in \mathbb{R}^N$.

To maintain pressures at desirable levels, water utilities use pumps on specific pipes. Let $\mathcal{P}_a \subset \mathcal{P}$ be the subset of pipes hosting a pump. The pipes in $\mathcal{P}_a$ can be considered lossless; this is without loss of generality since a pump can be modeled by an ideal pump followed by a short pipe. The remaining edges form the subset $\bar{\mathcal{P}}_a := \mathcal{P} \setminus \mathcal{P}_a$, and correspond to lossy pipes governed by (3). When pump $p = (m, n) \in \mathcal{P}_a$ is running, it adds pressure $g_{mn} \geq 0$ so that

$$h_n - h_m = g_{mn}.$$

The pressure added by a pump increases with the pump speed and decreases with the water flow through the pump. The exact relation is provided by manufacturers in the form of pump operation curves, and are oftentimes approximated with quadratic curve fits [21], [22], [8]. In detail, the pressure added by pump $p = (m, n)$ is modeled as

$$g_{mn}(f_{mn}, \omega_{mn}) = \lambda_{mn} f_{mn}^2 + \mu_{mn} \omega_{mn} f_{mn} + \nu_{mn} \omega_{mn}^2$$

where ω_{mn} is the pump speed; and $\lambda_{mn} < 0$, $\mu_{mn} \geq 0$, and $\nu_{mn} \geq 0$ are known pump parameters [8]. If pump (m, n) is running, its flow is constrained to lie within the range $0 \leq \underline{f}_{mn} \leq f_{mn} \leq \bar{f}_{mn}$ due to engineering limitations [20]. For a given pump speed ω_{mn}^0, the added pressure is

$$h_n - h_m = \lambda_{mn} f_{mn}^2 + \bar{\mu}_{mn} f_{mn} + \bar{\nu}_{mn} \quad (4)$$

where $\bar{\mu}_{mn} := \mu_{mn} \omega_{mn}^0$ and $\bar{\nu}_{mn} := \nu_{mn}(\omega_{mn}^0)^2$. Because the pump parameters satisfy $2\lambda_{mn}\underline{f}_{mn} + \mu_{mn}\omega_{mn} < 0$ over the operating range of pump speeds ω_{mn}, the pressure gain due to any pump is a *strictly decreasing function* of the water flow. This observation is instrumental in establishing the uniqueness of the WF solution in Section III.

When pump $p = (m, n) \in \mathcal{P}_a$ is not running, water can flow freely in either directions through a bypass valve [21], so that $g_{mn} = 0$ or $h_m = h_n$. In this case, the WDS graph can be reduced by removing pipe p and node n, and connecting to node m the edges previously incident to n.

Valves constitute a vital component for water flow control. They can be modeled by an on/off switch; a linear pressure-reducing model; a flow-dependent non-linear model; or a flow control model; see [8] and [12] for details. Under the typical operational setup, the valve at the reference node regulates pressure, whereas the valves in the remaining reservoirs and tanks regulate flows.

Summarizing this section, a WDS is described by the triplet $(\mathbf{d}, \mathbf{f}, \mathbf{h})$ satisfying the WF equations of (2)–(4). This work deals with the uniqueness of a WF solution and efficient solvers for finding this solution.

III. Uniqueness of Water Flow Solution

Different from the optimal water flow problem where tanks and pumps are scheduled over a time horizon, the WF task aims at solving the WF equations given the water injections $\mathbf{d}$. As such, it constitutes a key component of WDS operation and planning. The WF problem is formally stated next.

Definition 1. *Given: i) water injections $\mathbf{d}$; ii) the statuses and speeds $\{\omega_{mn}\}$ for all pumps $(m,n) \in \mathcal{P}_a$; and iii) the pressure h_r at the reference node $r \in \mathcal{N}$; the WF task aims at finding the flows $\mathbf{f}$ and pressures $\mathbf{h}$ satisfying (2)–(4).*

The WF task involves $N + P - 1$ equations over $N + P - 1$ unknowns. The water balance in (2) yields $N - 1$ linearly independent equations. In addition, the pressure drops across lossy pipes [cf. (3)], and the pressure gains due to pumps [cf. (4)] provide P non-linear equations. Although both $\mathbf{f}$ and $\mathbf{h}$ are unknown, it suffices to find any one of them: If $\mathbf{f}$ is known, then $\mathbf{h}$ can be calculated from (3)–(4) and h_r. On the other hand, if $\mathbf{h}$ is known, the flows $\mathbf{f}$ can be found thanks to the monotonicity of (3) and (4). Therefore, solving the WF task amounts to finding $\mathbf{f}$ or $\mathbf{h}$. Because this simple observation is used throughout our analysis, it is summarized as a lemma.

Lemma 1. *Given $\mathbf{d}$, a triplet $(\mathbf{d}, \mathbf{f}, \mathbf{h})$ satisfying (2)–(4) is uniquely characterized by $\mathbf{f}$ or $\mathbf{h}$.*

The WF task can be posed as the feasibility problem

$$\text{find} \quad \{\mathbf{f}, \mathbf{h}\} \tag{W1}$$
$$\text{s.to} \quad (2), (3), (4).$$

Since (3) and (4) are quadratic equality constraints, problem (W1) is non-convex. For a tree WDS graph $\mathcal{G}$ (for which $P = N - 1$), matrix $\mathbf{A}$ is square and invertible [23]. Then the flows $\mathbf{f}$ can be found uniquely from (2), and the WF task is readily solved according to Lemma 1. However, handling the WF task in a loopy $\mathcal{G}$ containing pumps remains non-trivial. Interestingly enough though, the next claim establishes the uniqueness of a WF solution regardless of the structure of $\mathcal{G}$ and the existence of pumps.

Theorem 1. *If the WF equations are feasible for some $\mathbf{d}$, they feature a unique solution.*

Proof: Proving by contradiction, assume $(\mathbf{h}, \mathbf{f})$ and $(\tilde{\mathbf{h}}, \tilde{\mathbf{f}})$ are two distinct solutions of (W1). Since the two flow vectors $\mathbf{f}$ and $\tilde{\mathbf{f}}$ satisfy (2), the vector $\mathbf{n} := \tilde{\mathbf{f}} - \mathbf{f}$ lies in the nullspace of $\mathbf{A}^\top$, that is $\mathbf{A}^\top \mathbf{n} = \mathbf{0}$. Then it follows that

$$\mathbf{n}^\top \mathbf{A}(\tilde{\mathbf{h}} - \mathbf{h}) = 0. \tag{5}$$

Let us decompose $\mathbf{n}$ into its positive and negative entries as $\mathbf{n} = \mathbf{n}_+ - \mathbf{n}_-$, where $\mathbf{n}_+ \geq \mathbf{0}$ and $\mathbf{n}_- \geq \mathbf{0}$. Plugging this decomposition into (5) yields

$$\mathbf{n}_+^\top \left(\mathbf{A}\tilde{\mathbf{h}} - \mathbf{A}\mathbf{h} \right) = \mathbf{n}_-^\top \left(\mathbf{A}\tilde{\mathbf{h}} - \mathbf{A}\mathbf{h} \right). \tag{6}$$

Recall from (3) that the pressure drop across a lossy pipe is monotonically increasing in flow. Similarly, the pressure added by a pump described by (4) is monotonically decreasing in flow. In other words, the pressure drop along a pump is
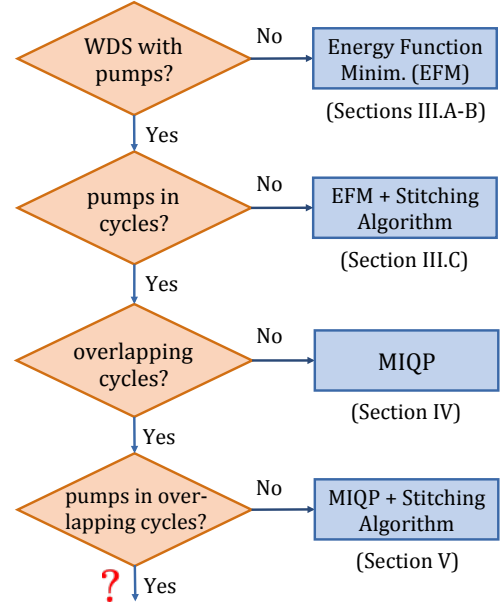

Fig. 1. Given a water distribution network, this flowchart suggests the most suitable WF solver based on its analytical guarantees and computational complexity.

monotonically increasing in flow. Therefore, for any edge $p \in \mathcal{P}$, it holds that

$$\mathbf{a}_p^\top \tilde{\mathbf{h}} > \mathbf{a}_p^\top \mathbf{h} \quad \text{if and only if} \quad \tilde{f}_p > f_p \tag{7}$$

where $\mathbf{a}_p^\top$ is the p-th row of matrix $\mathbf{A}$.

Consider the p-th entry of vector $\mathbf{n}$. If $\tilde{f}_p > f_p$, then $n_{+,p} > 0$ and $n_{-,p} = 0$ by definition of $\mathbf{n}_+$ and $\mathbf{n}_-$. Then edge p contributes to the left-hand side (LHS) of (6). The monotonicity in (7) entails that $\mathbf{a}_p^\top (\tilde{\mathbf{h}} - \mathbf{h}) > 0$ and so $n_{+,p} \cdot \mathbf{a}_p^\top (\tilde{\mathbf{h}} - \mathbf{h}) > 0$. The latter holds for all edges contributing to the LHS of (7), so that

$$\mathbf{n}_+^\top \left(\mathbf{A}\tilde{\mathbf{h}} - \mathbf{A}\mathbf{h} \right) > 0.$$

On the other hand, if $\tilde{f}_p < f_p$, then $n_{+,p} = 0$ and $n_{-,p} > 0$. Then, edge p contributes to the right-hand side (RHS) of (7). The monotonicity in (7) entails $n_{-,p} \cdot \mathbf{a}_p^\top (\tilde{\mathbf{h}} - \mathbf{h}) < 0$. Applying the claim over all edges participating in the RHS of (7) provides

$$\mathbf{n}_-^\top \left(\mathbf{A}\tilde{\mathbf{h}} - \mathbf{A}\mathbf{h} \right) < 0.$$

The signs of the LHS and RHS contradict the equality in (6), thus proving the claim. ∎

Regarding the pressure drop law of (3), the Hazen-Williams equation is sometimes used wherein the flow f_{mn} is raised to the exponent of 1.852. This exponent is different from the exponent of 2 in the Darcy-Weisbach equation; see for example [14]. While the Darcy-Weisbach equation is a theoretical formula, the Hazen-Williams equation is based on curve fitting of experimental data [5]. Nevertheless, the uniqueness argument of Theorem 1 holds for any positive exponent on the water flow involved in the pressure drop equation.

Having established the uniqueness of the WF solution, the ensuing sections develop a suite of WF solvers of complementary value: Each solver finds provably the WF solution under a

different network setup. The devised solvers exhibit different computational complexity, yet none of them requires a proper initialization. Figure 1 summarizes the particular WDS setups each solver can handle, and serves as a roadmap for the following sections.

IV. ENERGY FUNCTION-BASED WATER FLOW SOLVERS

The WF task for networks without pumps is posed here as a constrained convex minimization (Section IV-A), and an equivalent unconstrained convex minimization (Section IV-B). The approach is then generalized to networks with pumps, but not on cycles (Section IV-C).

A. Constrained Formulation

For a WDS without pumps, the WF task simplifies to solving (2)–(3). These two equations are structurally similar to the equations governing the flows and pressures in a natural gas network under steady-state conditions [24]. Exploiting this link and adopting the energy function minimization approach for solving the gas flow equations in [25], we next pose (W1) as a constrained minimization over $\mathbf{f}$.

Lemma 2. *In a WDS without pumps ($\mathcal{P} = \bar{\mathcal{P}}_a$), the vector of water flows $\mathbf{f}$ satisfying (2)–(3) can be found as the unique minimizer of the convex minimization problem*

$$\min_{\mathbf{f}} \quad \frac{1}{3} \sum_{p \in \mathcal{P}} c_p |f_p|^3 \tag{8a}$$

$$\text{s.to} \quad \mathbf{A}^\top \mathbf{f} = \mathbf{d}. \tag{8b}$$

Moreover, if $\boldsymbol{\xi}^*$ is the vector of optimal Lagrange multipliers corresponding to (8b), then the nodal pressures are provided by $\mathbf{h} = (\mathbf{I} - \mathbf{1}\mathbf{e}_r^\top)\boldsymbol{\xi}^* + h_r\mathbf{1}$.

Proof: The objective function of (8) can be written as the ℓ_3-norm of a scaled flow vector raised to the third power. Its strict convexity follows from composition rules [26, Sec. 3.2.4]. Then, the uniqueness of the minimizer of (8) stems from strong convexity. Moreover, the objective is differentiable: the p-th entry of its gradient vector $\mathbf{g}_c(\mathbf{f})$ is $c_p \operatorname{sign}(f_p)|f_p|^2$.

The Lagrangian function associated with (8) is

$$L(\mathbf{f}; \boldsymbol{\xi}) = \frac{1}{3} \sum_{p \in \mathcal{P}} c_p |f_p|^3 + \boldsymbol{\xi}^\top (\mathbf{d} - \mathbf{A}^\top \mathbf{f}). \tag{9}$$

The optimal primal and dual variables $(\mathbf{f}^*, \boldsymbol{\xi}^*)$ satisfy the Lagrangian optimality condition, that is $\mathbf{g}_c(\mathbf{f}^*) = \mathbf{A}\boldsymbol{\xi}^*$, which coincides with (3).

By the definition of $\mathbf{A}$ in (1), it holds that $\mathbf{A}\boldsymbol{\xi}^* = \mathbf{A}(\boldsymbol{\xi}^* + \alpha \mathbf{1})$ for any $\alpha \in \mathbb{R}$. Hence, the pressures can be recovered either by Lemma 1, or by fixing $\alpha = h_r - \mathbf{e}_r^\top \boldsymbol{\xi}^*$ to equate the r-th entry of $\boldsymbol{\xi}^* + \alpha \mathbf{1}$ to the reference pressure h_r. ∎

Lemma 2 provides a computational tool for solving the WF equations in water networks without pumps. It further shows that the WF solution is unique in networks without pumps. This claim has also been established using a contraction argument in [14]. It is worth mentioning that Theorem 1 generalizes this uniqueness claim to water networks containing pumps.

The problem in (8) can be solved by reformulating it to the second-order cone program (SOCP)

$$\min_{\{f_p, w_p, y_p, t_p\}} \quad \frac{1}{3} \sum_{p \in \mathcal{P}} c_p t_p \tag{10a}$$

$$\text{s.to} \quad \mathbf{A}^\top \mathbf{f} = \mathbf{d}. \tag{10b}$$

$$- w_p \leq f_p \leq w_p, \qquad \forall p \tag{10c}$$

$$w_p^2 \leq y_p, \ y_p^2 \leq w_p t_p, \qquad \forall p. \tag{10d}$$

The equivalence can be established by showing that the minimizers of (10) satisfy $w_p = |f_p|$; $y_p = w_p^2 = f_p^2$; and $t_p = w_p^3 = |f_p|^3$ for all $p \in \mathcal{P}$. Each constraint in (10d) constitutes a rotated second-order cone. A similar SOCP reformulation of the WF equations has been previously adopted in [8] and [27] for solving an optimal water flow problem.

Alternatively, problem (8) can be tackled via the iterative method of dual decomposition: During the k-th iteration, the primal variable $\mathbf{f}$ is updated by minimizing the Lagrangian function $L(\mathbf{f}; \boldsymbol{\xi}^k)$ evaluated at the latest estimate of dual variables $\boldsymbol{\xi}^k$. The latter problem decouples across pipes as

$$f_p^{k+1} := \arg\min_{f_p} \frac{1}{3} c_p |f_p|^3 - f_p \mathbf{a}_p^\top \boldsymbol{\xi}^k$$

whose minimizer is provided in closed-form

$$f_p^{k+1} = \operatorname{sign}(\mathbf{a}_p^\top \boldsymbol{\xi}^k) \sqrt{\frac{|\mathbf{a}_p^\top \boldsymbol{\xi}^k|}{c_p}}. \tag{11}$$

Then, for a step-size $\mu > 0$, the dual variables are updated as

$$\boldsymbol{\xi}^{k+1} := \boldsymbol{\xi}^k + \mu \left(\mathbf{d} - \mathbf{A}^\top \mathbf{f}^{k+1} \right).$$

B. Unconstrained Formulation

For a WDS without pumps, Section IV-A formulated the WF task as a constrained minimization over the flow vector $\mathbf{f}$. The same WF task can be alternatively posed as an *unconstrained* minimization over the pressure vector $\mathbf{h}$

$$\min_{\mathbf{h}} \quad \frac{2}{3} \sum_{(m,n) \in \mathcal{P}} \frac{|h_m - h_n|^{\frac{3}{2}}}{\sqrt{c_{mn}}} - \mathbf{d}^\top \mathbf{h}. \tag{12}$$

The objective of (12) is convex (again by composition rules) and differentiable. The n-th entry of its gradient vector $\mathbf{g}_u(\mathbf{h})$ is

$$[\mathbf{g}_u(\mathbf{h})]_n = \sum_{p=(m,n) \in \mathcal{P}} \operatorname{sign}(\mathbf{a}_p^\top \mathbf{h}) \sqrt{\frac{|\mathbf{a}_p^\top \mathbf{h}|}{c_p}} - d_n.$$

Setting this gradient equal to zero yields the WF equations after eliminating $\mathbf{f}$ from (2)–(3). The ambiguity in pressures can be waived by shifting the minimizer of (12) to match the reference pressure h_r. Once the pressures $\mathbf{h}$ have been found, the flow vector $\mathbf{f}$ can be retrieved by Lemma 1. Problem (12) is amenable to any first-order method for unconstrained optimization, such as the gradient descent iterations $\mathbf{h}^{k+1} := \mathbf{h}^k - \mu \mathbf{g}_u(\mathbf{h}^k)$ for a step-size $\mu > 0$, or accelerated variants.

Remark 1. *Let us compare the costs of* (8) *and* (12). *Due to* (3), *it holds that* $c_p f_p^2 = |\mathbf{a}_p^\top \mathbf{h}|$ *and* $\mathrm{sign}(f_p) = \mathrm{sign}(\mathbf{a}_p^\top \mathbf{h})$. *Therefore, the cost in* (8) *can be rewritten as*

$$\frac{1}{3} \sum_{p \in \mathcal{P}} |f_p \cdot \mathbf{a}_p^\top \mathbf{h}|. \tag{13}$$

Likewise, the first summand of the cost in (12) *becomes*

$$\frac{2}{3} \sum_{p \in \mathcal{P}} |f_p \cdot \mathbf{a}_p^\top \mathbf{h}|. \tag{14}$$

The product of pressure drop times water flow captures exactly the energy lost across a pipe; see also [8] and [27]. Therefore, problem (8) *finds the* $\mathbf{f}$ *that minimizes friction losses for a given* $\mathbf{d}$; *hence, the term 'energy function minimization.' While water demands* $\mathbf{d}$ *appear in the constraint of* (8), *their effect is incorporated in* (12) *via the* $-\mathbf{d}^\top \mathbf{h}$ *component of the cost. As commented in [8], the product* $-d_n h_n$ *yields the power lost in delivering demand* d_n *under pressure* h_n *at node* n. *Thus, problem* (12) *minimizes the energy lost in pipes and in serving demands. Energy function-based approaches have been used traditionally for studying the stability of electric power systems [28], [29]; and recently for establishing the uniqueness of electric power [30], [31], and natural gas flow equations [24], [25].*

C. Extension to WDS with no Pumps in Cycles

Since problems (8) and (12) cannot handle water networks with pumps, this section extends their applicability to networks with pumps, but not on cycles. This is accomplished by adopting the reduction technique of [32] to build what we term *stitching algorithm*:

S1) Remove the edges of $\mathcal{G}$ corresponding to pumps $\mathcal{P}_a$. The obtained graph contains $|\mathcal{P}_a| + 1$ disconnected components $\mathcal{G}_c$ for $c = 1, \ldots, |\mathcal{P}_a| + 1$.

S2) Replace each component $\mathcal{G}_c$ by a supernode, and connect the supernodes using the edges in $\mathcal{P}_a$ to create the supergraph $\mathcal{G}'$. Graph $\mathcal{G}'$ features a *tree structure*.

S3) Find the total water injection per supernode $\mathcal{G}_c$. Since $\mathcal{G}'$ is a tree, the water flows on $\mathcal{P}_a$ can be found readily.

S4) If the flow along pump $(m, n) \in \mathcal{P}_a$ is f_{mn}, modify the injections at nodes m and n as $\hat{d}_m = d_m - f_{mn}$ and $\hat{d}_n = d_n + f_{mn}$.

S5) Solve (8) per connected component $\mathcal{G}_c$ to find the water flows at all lossy pipes.

S6) Having acquired vector $\mathbf{f}$, the pressure vector $\mathbf{h}$ can be found from Lemma 1.

In *S5)*, rather than solving the constrained minimization of (8), one could use its unconstrained counterpart of (12). Steps *S1)–S4)* are still needed to find a meaningful water injection vector per component $\mathcal{G}_c$. Once a pressure vector has been found per component, the pressures must be revised as follows: The pressures within the component containing the reference node, say component $\mathcal{G}_1$, are kept unaltered. Consider a pump running from node $m \in \mathcal{G}_1$ to node $n \in \mathcal{G}_2$. Having found h_m by solving (12) in $\mathcal{G}_1$, the pressure at node n should be $h_n = h_m + g_{mn}$, where the flow f_{mn} has been found in step *S3)*. If the pressure at node n recovered by solving (12)

in $\mathcal{G}_2$ is $\tilde{h}_n$, then all pressures within $\mathcal{G}_2$ should be shifted by $h_n - \tilde{h}_n$. The process is repeated for all components to recover the entire pressure vector $\mathbf{h}$.

To broaden the applicability of our WF solvers to networks with pumps in cycles, we next pursue an MIQP solver.

V. MIQP WATER FLOW SOLVER

This section presents an MIQP relaxation of (W1) along with sufficient conditions for its exactness.

A. Problem Reformulation

The non-convexity of the WF problem (W1) is due to constraints (3) and (4). These quadratic equalities can be relaxed to convex inequality constraints: The pressure drop along pipe $(m, n) \in \bar{\mathcal{P}}_a$ is relaxed from (3) to

- $h_m - h_n \geq c_{mn} f_{mn}^2$ for $f_{mn} \geq 0$; or
- $h_n - h_m \geq c_{mn} f_{mn}^2$ for $f_{mn} \leq 0$.

To handle the two cases, let us introduce a binary variable x_{mn} capturing the flow direction on pipe (m, n). By using the so-termed big-M trick, the two cases can be modeled as

$$-M(1 - x_{mn}) \leq f_{mn} \leq M x_{mn} \tag{15a}$$
$$-M(1 - x_{mn}) \leq h_m - h_n - c_{mn} f_{mn}^2 \tag{15b}$$
$$h_m - h_n + c_{mn} f_{mn}^2 \leq M x_{mn} \tag{15c}$$
$$x_{mn} \in \{0, 1\}. \tag{15d}$$

Constraint (15a) implies that $x_{mn} = \mathrm{sign}(f_{mn})$. If $x_{mn} = 1$, the convex quadratic constraint in (15b) is activated, whereas constraint (15c) becomes trivial. The claim reverses for $x_{mn} = 0$. Depending on the value x_{mn}, if either (15b) or (15c) is satisfied with equality, the relaxation is deemed as *exact*. If that happens for all lossy pipes, the feasible set of (15) has captured the original non-convex constraints in (3).

Similarly, the pressure added by pump $(m, n) \in \mathcal{P}_a$ is relaxed from (4) to

$$h_n - h_m \leq \lambda_{mn} f_{mn}^2 + \hat{\mu}_{mn} f_{mn} + \hat{\nu} \tag{16}$$

which is a convex constraint since $\lambda_{mn} < 0$. Again, if the inequality in (16) is satisfied with equality for all pumps, the relaxation of (4) to (16) is deemed as exact.

One may now try solving (W1) upon replacing (3) and (4) respectively by (15) and (16). If all the relaxed constraints are satisfied with equality, the relaxation is exact. Of course that is not guaranteed. To favor exact relaxations, we convert the feasibility to a minimization problem with a judiciously selected cost. We thus arrive at the MIQP formulation

$$\min \quad s(\mathbf{h}) \tag{W2}$$
$$\text{over} \quad \mathbf{f}, \mathbf{h}, \mathbf{x}$$
$$\text{s.to} \quad (2), (15), (16)$$

where the binary vector $\mathbf{x}$ contains all $\{x_{mn}\}_{(m,n) \in \bar{\mathcal{P}}_a}$, and the cost is defined as

$$s(\mathbf{h}) := \sum_{(m,n) \in \bar{\mathcal{P}}_a} |h_m - h_n| - \sum_{(m,n) \in \mathcal{P}_a} (h_n - h_m).$$

The cost sums up the absolute pressure drops across lossy pipes minus the pressure gains added by pumps. A related

MI-SOCP relaxation has been proposed for an instance of the optimal water flow (OWF) problem [9]. In that work, the absolute pressure drops across lossy pipes is appended as a penalty to the objective of the OWF problem. Adding this penalty renders the relaxation exact under some sufficient conditions. Although the conditions are restrictive, in practice this OWF relaxation turns out to be numerically exact under practical water networks [9].

Problem (W2) is non-convex due to the binary variables **x**. However, given the advancements in MIQP solvers, this minimization can be handled for moderately sized networks [33]. Recall that every lossy pipe is associated with a binary and a continuous optimization variable. To accelerate the computations, we next provide a simple pre-processing step to determine the flows in all edges not belonging to a cycle.

Lemma 3. *Let* **f** *be the unique flow solution of* (W1)*, and consider any vector* $\tilde{\mathbf{f}}$ *satisfying* $\mathbf{A}^\top \tilde{\mathbf{f}} = \mathbf{d}$*. For any edge* (m,n) *not belonging to a cycle, it holds that* $\tilde{f}_{mn} = f_{mn}$*.*

Proof: Consider the minimum-norm solution $\mathbf{f}_0 := (\mathbf{A}^\top)^\dagger \mathbf{d}$ to the linear system of (2), where $(\mathbf{A}^\top)^\dagger$ is the pseudo-inverse of $\mathbf{A}^\top$. Any other solution of (2) can be expressed as $\mathbf{f} = \mathbf{f}_0 + \mathbf{n}$ for some vector $\mathbf{n} \in \text{null}(\mathbf{A}^\top)$.

The space $\text{null}(\mathbf{A}^\top)$ can be represented using the cycles of graph $\mathcal{G}$ as explained next. For cycle $\mathcal{C}$ in $\mathcal{G}$, select an arbitrary direction and define its indicator vector $\mathbf{n}_\mathcal{C} \in \mathbb{R}^P$ as

$$n_{\mathcal{C},p} := \begin{cases} 0 & \text{, if edge } p \notin \mathcal{C} \\ +1 & \text{, if the directions of } p \text{ and } \mathcal{C} \text{ coincide} \\ -1 & \text{, otherwise.} \end{cases}$$

We are particularly interested in a set of *fundamental cycles* defined as follows [23]: In graph $\mathcal{G} = (\mathcal{N}, \mathcal{P})$, select a spanning tree $\mathcal{T}$. Every edge $p \in \mathcal{P} \setminus \mathcal{T}$ along with some edges of $\mathcal{T}$ form a cycle. The cycles formed using all edges in $\mathcal{P} \setminus \mathcal{T}$ comprise the set $\mathcal{L}_\mathcal{T}$ of fundamental cycles.

A key property of fundamental cycles is that the space $\text{null}(\mathbf{A}^\top)$ is spanned by the indicator vectors for any set of fundamental cycles [23, Corollary 14.2.3]. Therefore, the vector $\mathbf{n}$ in $\mathbf{f} = \mathbf{f}_0 + \mathbf{n}$ can be decomposed as

$$\mathbf{n} = \sum_{\ell \in \mathcal{L}_\mathcal{T}} \alpha_\ell \mathbf{n}_\ell \tag{17}$$

where $\mathbf{n}_\ell$ is the indicator vector for cycle ℓ and $\alpha_\ell \in \mathbb{R}$.

Consider the p-th entry of $\mathbf{n}$. If edge $p \in \mathcal{P}$ does not belong to any cycle, then it does not belong to any fundamental cycle. Then $n_{\ell,p} = 0$ for all $\ell \in \mathcal{L}_\mathcal{T}$, and $n_p = 0$ follows from (17). To conclude, if edge p does not belong to a cycle, then all solutions $\mathbf{f}$ of (2) agree in their p-th entry. ∎

Lemma 3 ensures that for weekly meshed WDS, the number of variables in (W2) can be reduced markedly. Moreover, the flow on any edge not belonging to a cycle coincides with the related entry of the minimum-norm solution to (2).

B. Exactness of the Relaxation

The next result shown in the appendix provides conditions under which a minimizer of (W2) satisfies (15)–(16) with equality.
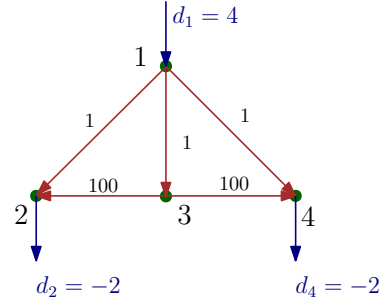

Fig. 2. A pathological WDS for which the relaxation of (W2) is inexact.

Theorem 2. *In a WDS where no edge* $(m,n) \in \mathcal{P}$ *belongs to more than one cycle, a minimizer of* (W2) *minimizes* (W1) *as well, if* (W1) *is feasible.*

Theorem 2 asserts that the MIQP relaxation of (W1) to (W2) is exact in water networks with non-overlapping cycles, that is cycles sharing at least one edge. The claim holds regardless of water demand or the presence of pumps; yet its network condition may not always hold. Nonetheless, the numerical tests of Section VII demonstrate that the relaxation is exact and (W2) solves the WF problem for practical WDS exhibiting overlapping cycles.

The condition imposed by Theorem 2 cannot be analytically relaxed: One could construct pathological examples of water networks with overlapping cycles that render the relaxation of (W2) inexact; such a counterexample is presented next. Consider the 4-node and 5-pipe water network of Figure 2. The coefficients c_{mn}'s are shown on the respective pipes. Nodes 2 and 4 host water demands, and the reference node 1 supplies water at the reference pressure of $h_1 = 10$. The edge $(1,3)$ belongs to two cycles and hence the condition of Theorem 2 is violated. The minimizer of (W2) satisfies the relaxed constraint (15) with strict inequality. The pressure at nodes 1 and 3 were found to differ by $h_1 - h_3 = 3.435$, while the frictional drop was $c_{13}f_{13}^2 = 0.014$. This WDS however is characterized by a strong disparity of pipe coefficients. For a WDS with limited variations in pipe dimensions and material, such disparity is not anticipated in practice.

Since the WDS of Figure 2 does not host pumps, the solution to the previous WF problem was eventually found using the energy function minimization approach of (8). This motivates us to exploit the ability of the energy function-based approach to handle overlapping cycles alongside the merit of the MIQP relaxation to handle pumps in cycles. To solve the WF problem for a broader class of WDS network topologies, a hybrid solver is developed next.

VI. HYBRID WATER FLOW SOLVER

The hybrid WF solver relaxes the assumption of non-overlapping cycles of Theorem 2 to the following condition.

Assumption 1. *The water network has no pumps in overlapping cycles.*

The assumption permits overlapping cycles, but these particular cycles should carry no pumps. For a network satisfying

Assumption 1, the WF task can be solved through the following steps illustrated also in Figure 3:

T1) Any cycle $\mathcal{C}$ with pumps is non-overlapping. Thus, for any node n belonging to $\mathcal{C}$, two cases arise:
i) Node n belongs only to cycle $\mathcal{C}$ (node 3 of $\mathcal{C}_1$); or
ii) Node n belongs to other cycle(s) $\mathcal{C}'$ as well; yet $\mathcal{C}$ and $\mathcal{C}'$ share no edge (e.g., node 4 of $\mathcal{C}_2$).
Then, reduce graph $\mathcal{G}$ to $\mathcal{G}'$ through the steps:
- If for a cycle $\mathcal{C}$ having pumps, all nodes do not belong to any other cycle, replace $\mathcal{C}$ by a supernode $n_{\mathcal{C}}$.
- If for a cycle $\mathcal{C}$ having pumps, node n belongs to other cycle(s), identify the edges (n_1, n) and (n, n_2), which belong to $\mathcal{C}$. These two edges belong to no other cycles as $\mathcal{C}$ is non-overlapping. Split the node n into n and n' connected by a lossless edge (n, n'), such that all edges in $\mathcal{G}$ other than (n_1, n) and (n, n_2) that were incident on n are now incident on n'. After repeating this step for all nodes in $\mathcal{C}$ that belong to multiple cycles, replace $\mathcal{C}$ by a supernode $n_{\mathcal{C}}$.

This process ensures that in $\mathcal{G}'$ all supernodes and the pumps left out from $\mathcal{G}$ do not appear on cycles.

T2) Use Lemma 3 to compute the water flows on the edges $(m, n_{\mathcal{C}})$ incident to supernodes $n_{\mathcal{C}}$'s in $\mathcal{G}'$.
T3) For each edge $(m, n_{\mathcal{C}})$ in $\mathcal{G}'$, modify the injection at node m as $\hat{d}_m = d_m - f_{mn_{\mathcal{C}}}$.
T4) Partition $\mathcal{G}'$ into a set of connected components $\mathcal{G}_c$ by removing the supernodes and their incident edges. Each $\mathcal{G}_c$ has known injections and bears no pumps in cycles.
T5) Use the stitching algorithm of Section IV-C per component $\mathcal{G}_c$ to find the flows within $\mathcal{G}_c$.
T6) Each supernode $n_{\mathcal{C}}$ is split back to the cycle $\mathcal{C}$ it replaced. If the edge $(m, n_{\mathcal{C}})$ of $\mathcal{G}'$ corresponded to edge (m, n) of $\mathcal{G}$, modify the injection at node $n \in \mathcal{C}$ as $\hat{d}_n = d_n + f_{mn_{\mathcal{C}}}$.
T7) Solve (W2) per cycle $\mathcal{C}$ to find the water flows on $\mathcal{C}$.
T8) Given vector $\mathbf{f}$, find the pressure vector $\mathbf{h}$ using Lemma 1.

Let us apply the previous steps on the 23-node and 28-pipe water network of Figure 3. There are two cycles carrying pumps, marked as $\mathcal{C}_1$ and $\mathcal{C}_2$. Node 4 of cycle $\mathcal{C}_1$ belongs to multiple cycles and hence it is split in 4 and 4'. Next, removing $\mathcal{C}_1$ and $\mathcal{C}_2$ along with the edges that connect these cycles with the rest of the graph results in the connected subgraphs $\mathcal{G}_1$, $\mathcal{G}_2$, and $\mathcal{G}_3$ shown on the bottom of Figure 3. The demands on boundary nodes are modified as per steps *T3)* and *T6)*. The edge flows within each connected component are subsequently found by solving (8). The flows on $\mathcal{C}_1$ and $\mathcal{C}_2$ are finally found by (W2).

This WDS setup could not be handled by the energy function-based approach of Section IV alone due to the presence of pumps on cycles $\mathcal{C}_1$ and $\mathcal{C}_2$. The convex relaxation of Section V alone is not guaranteed to succeed either, due to the presence of overlapping cycles. Combining the merits of each method and leveraging Lemma 3, this hybrid method can handle successfully this WDS setup.

VII. NUMERICAL TESTS

The new WF solvers were evaluated on the EPANET *Example Network-2* representing a water network from Cherry Hills,
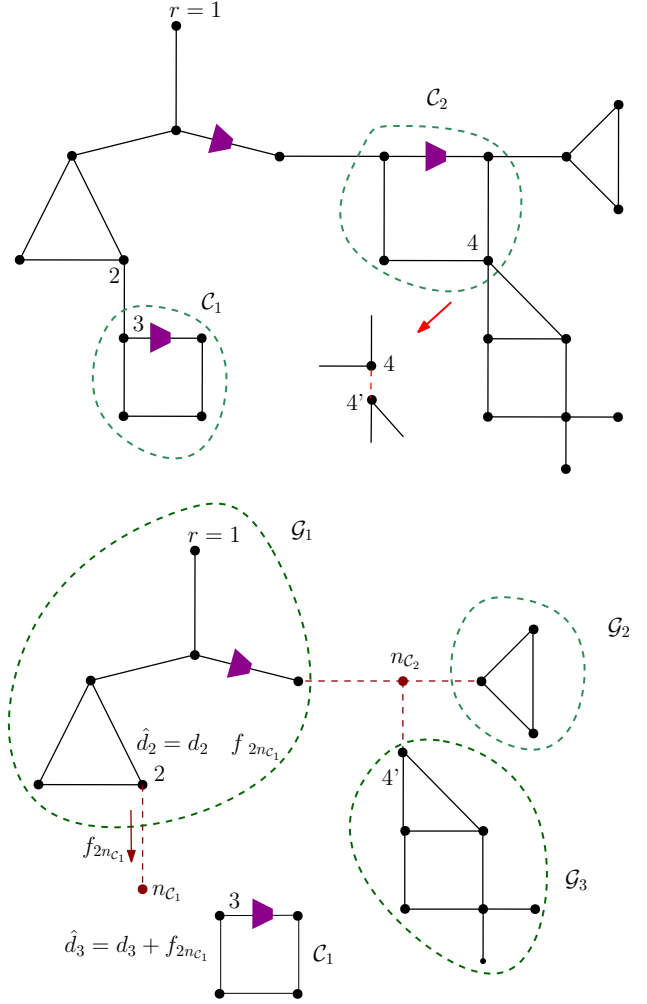

Fig. 3. *Top:* A water distribution network with pumps in non-overlapping cycles; *Bottom*: Connected components after removing cycles $\mathcal{C}_1$ and $\mathcal{C}_2$ that carry pumps.

Connecticut [3], and is shown in Fig. 4. This network consists of $P = 40$ pipes, $N = 34$ demand nodes, one tank, and one pump station. We modified the network by representing the pump station as a reservoir with pressure 100ft connected to a fixed-speed pump with a head gain of 100 ft. All nodes were assumed to be at the same reference elevation. The pipe friction coefficients c_{mn}'s, tank dimensions, and base demand vector $\mathbf{d}$, were derived from the EPANET benchmark.

We first tested whether the proposed solvers yield a WF solution that agrees with the EPANET solution. For this purpose, we obtained WF solutions using the constrained energy function minimization of (8) and the MIQP solver (W2). Problem (8) was solved using the closed-form dual decomposition steps of Section IV-A with $\mu = 10^{-4}$ and $20,000$ iterations. The MIQP in (W2) was solved using the MATLAB-based toolbox YALMIP along with the mixed-integer solver CPLEX [34], [35]. All tests were run on a 2.7 GHz, Intel Core i5 computer with 8 GB RAM. The flows obtained by the two solvers were very close to the EPANET solution, as illustrated in Figure 5; EPANET uses more detailed flow models, e.g., the coefficient c_{mn} in (3)
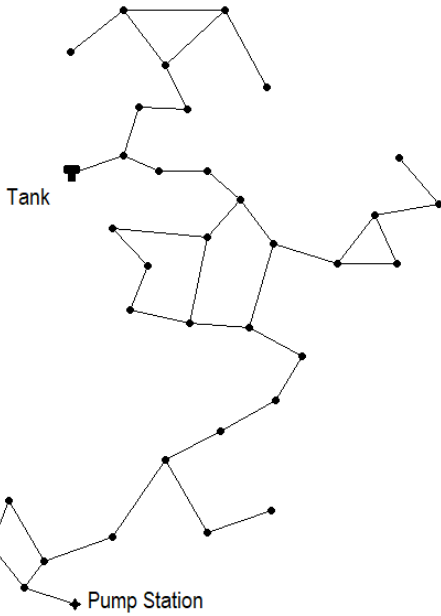
Fig. 4. EPANET Example Network-2 of a water distribution system from Cherry Hills, CT [3].
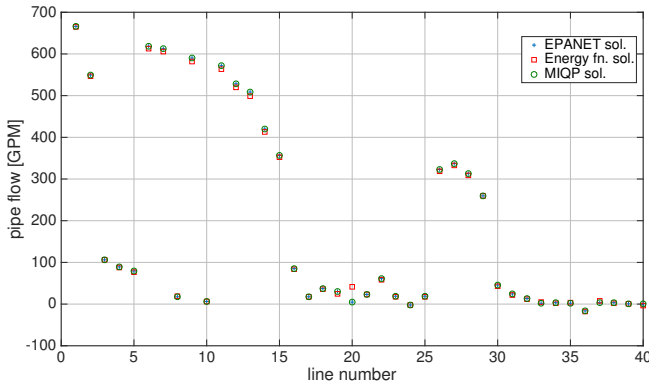

Fig. 5. Water flows obtained by the EPANET solver, the constrained energy function minimization of (8), and the MIQP of (W2) for the network of Fig. 4.

depends weakly on flow f_{mn}. The $20,000$ iterations for the primal-dual updates of (8) were completed within 4.5 sec, and the running time of the MIQP (W2) was 1.6 sec.

Finally, we evaluated the performance of the (W2) solver in finding the correct WF solution, when the conditions of Theorem 2 are not satisfied. Specifically, the network of Figure 4 has overlapping cycles. To represent various demand levels, we generated 100 random WF instances by scaling the base demand $\mathbf{d}$ for the EPANET network by a scalar uniformly drawn from $[0, 1.5]$. Given a minimizer of (W2), we defined the inexactness over lossy pipe (m, n) as $|h_m - h_n| - c_{mn} f_{mn}^2$. For each run of (W2) with a random input, the ranked maximum inexactness gap over all lossy pipes is displayed on Figure 6 (top). Despite violating the conditions of Theorem 2, the maximum inexactness gap is small for all random tests. On the computational side, the running time of the MIQP-based solver of (W2) over the 100 instances is shown in the bottom panel of Figure 6; its median
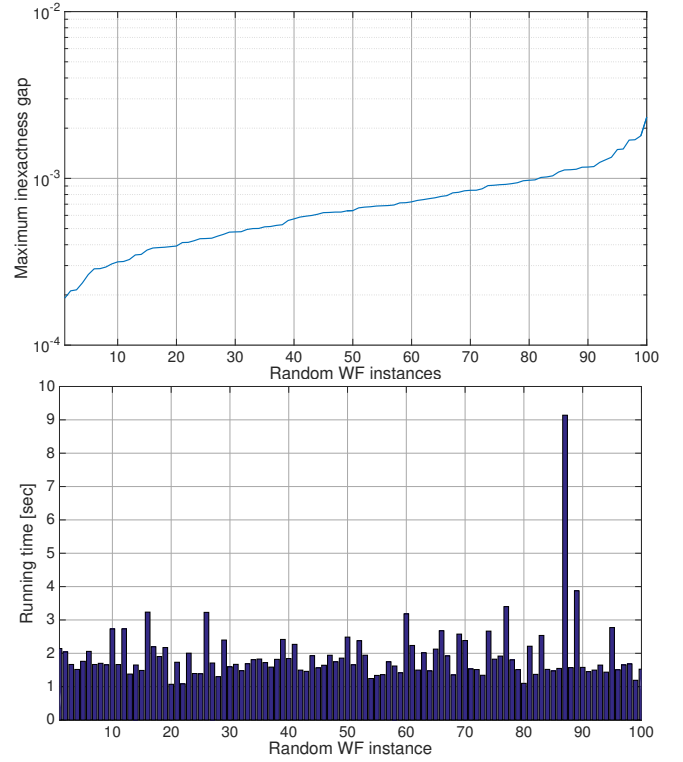

Fig. 6. *Top:* Maximum inexactness gap attained by (W2) over 100 random WF instances. *Bottom*: Running time for (W2) over random WF instances.

value was only 1.68 sec.

VIII. CONCLUSIONS

Using recent tools from graph theory, convex relaxations, energy function-based approaches, and mixed-integer programing, this work has provided a fresh perspective on the physical laws governing water distribution networks. It has been established that the WF problem admits a unique solution even in networks with pumps. Given water demands, this WF solution can be provably recovered via a hierarchical stack of WF solvers suitable for different network configurations. Radial networks can be handled by simple convex minimization tasks, whereas networks with cycles call for more elaborate MIQP-based solvers. Nevertheless, numerical tests demonstrate that even the MIQP approach scales well for moderately-sized networks. The MIQP solvers have been derived upon a convex relaxation of the pressure drop equation followed by an objective penalization, an approach that sparked a parallel line of research on the OWF problem [9]. Network configurations hosting pumps on overlapping cycles remain to be a challenging case. Moreover, solving the WF equations given a different set of parameters, such as a mixture of water injections, wtare flows, and/or nodal pressures, constitutes a pertinent computational problem.

APPENDIX

Proof of Theorem 2: The cost of (W2) can be written as

$$s(\mathbf{h}; \mathbf{f}) = \sum_{(m,n)\in\mathcal{P}} (h_m - h_n)\operatorname{sign}(f_{mn}).$$

To express pressure differences along the flow direction in a compact manner, define the $P \times N$ edge-node incidence matrix $\mathbf{A}(\mathbf{f})$: Its dependence on $\mathbf{f}$ signifies that the directionality of each edge coincides with the flow directions in $\mathbf{f}$. Therefore, if the p-th row of $\mathbf{A}(\mathbf{f})$ is associated with pipe $p = (m, n)$, then its (p, k) entry is

$$A_{p,k}(\mathbf{f}) := \begin{cases} -\operatorname{sign}^2(f_{mn}) + \operatorname{sign}(f_{mn}) + 1 & , \ k = m \\ \operatorname{sign}^2(f_{mn}) - \operatorname{sign}(f_{mn}) - 1 & , \ k = n \\ 0 & , \ \text{otherwise.} \end{cases}$$

For zero flows $(\operatorname{sign}(f_{mn}) = 0)$, the default pipe direction (m, n) is selected without loss of generality.

Based on $\mathbf{A}(\mathbf{f})$, the pressure differences along the direction of flows can be written as $\mathbf{A}(\mathbf{f})\mathbf{h}$, and so

$$s(\mathbf{h}; \mathbf{f}) = \mathbf{1}^\top \mathbf{A}(\mathbf{f})\mathbf{h}. \tag{18}$$

If (W1) is feasible, denote its unique solution by $(\mathbf{f}, \mathbf{h})$. Proving by contradiction, suppose $(\tilde{\mathbf{f}}, \tilde{\mathbf{h}})$ is a minimizer of (W2), which is not feasible for (W1). Let us simplify notation as $\mathbf{A}(\mathbf{f}) := \mathbf{A}$ and $\mathbf{A}(\tilde{\mathbf{f}}) := \tilde{\mathbf{A}}$. Since both $\mathbf{f}$ and $\tilde{\mathbf{f}}$ satisfy (2), there exists a nonzero vector $\mathbf{n} \in \operatorname{null}(\mathbf{A}^\top)$ such that

$$\tilde{\mathbf{f}} = \mathbf{f} + \mathbf{n}. \tag{19}$$

As showed in (17), the vector $\mathbf{n}$ can be expressed in terms of a set $\mathcal{L}_\mathcal{T}$ of fundamental cycles.

Building on (17), consider the p-th entry of $\mathbf{n}$. Because edge p belongs to at most one cycle, either $n_p = 0$ or $n_p = \alpha_\ell n_{\ell,p}$ for a single $\ell \in \mathcal{L}$. In the latter case, if $\alpha_\ell < 0$, then one can reverse the direction of cycle ℓ and substitute $(\alpha_\ell, \mathbf{n}_\ell)$ in (17) with $(-\alpha_\ell, -\mathbf{n}_\ell)$. Hence, it can be assumed that $\alpha_\ell \geq 0$ for all $\ell \in \mathcal{L}$ without loss of generality.

Each vector $\mathbf{n}_\ell$ can be decomposed as $\mathbf{n}_\ell = \mathbf{n}_\ell^+ - \mathbf{n}_\ell^-$, where $\mathbf{n}_\ell^+ := \max\{\mathbf{n}_\ell, \mathbf{0}\}$ and $\mathbf{n}_\ell^- := \max\{-\mathbf{n}_\ell, \mathbf{0}\}$. Because every edge belongs to at most one cycle, it holds that

$$\mathbf{1} = \sum_{\ell \in \mathcal{L}} \mathbf{n}_\ell^+ + \sum_{\ell \in \mathcal{L}} \mathbf{n}_\ell^- + \mathbf{n}^0 \tag{20}$$

where the p-th entry of vector $\mathbf{n}^0$ is 1 if edge p does not belong to any cycle; and 0, otherwise. Using (20) in (18), the objective function of (W2) becomes

$$s(\mathbf{h}; \mathbf{f}) = \sum_{\ell \in \mathcal{L}} (\mathbf{n}_\ell^+)^\top \mathbf{A}\mathbf{h} + \sum_{\ell \in \mathcal{L}} (\mathbf{n}_\ell^-)^\top \mathbf{A}\mathbf{h} + (\mathbf{n}^0)^\top \mathbf{A}\mathbf{h}. \tag{21}$$

Although the function $s(\mathbf{h}; \mathbf{f})$ will be evaluated for different pairs $(\mathbf{h}; \mathbf{f})$, the vectors $\mathbf{n}_\ell$'s remain unchanged and depend on $\mathbf{A}$. Based on (17) and (21), we will next show that $s(\mathbf{h}; \mathbf{f}) < s(\tilde{\mathbf{h}}; \tilde{\mathbf{f}})$. To do so, we consider the three terms of (21) separately.

First summand of (21). Recall $\mathbf{n}_\ell^+$ is a binary vector. If $n_{\ell,p}^+ = 1$, then $\tilde{f}_p = f_p + \alpha_\ell \geq f_p \geq 0$. In that case, if edge p runs from node m to node n and corresponds to a lossy pipe, we get that

$$(\tilde{h}_m - \tilde{h}_n)\operatorname{sign}(\tilde{f}_p) \geq c_{mn}\tilde{f}_p^2$$
$$\geq c_{mn}f_p^2$$
$$= (h_m - h_n)\operatorname{sign}(f_p) \tag{22}$$

where the first inequality stems from constraint (15) of (W2); the second one from $\tilde{f}_p \geq f_p \geq 0$; and the equality from constraint (3) of (W1).

If edge p corresponds to a pump, we can similarly show

$$(\tilde{h}_m - \tilde{h}_n)\operatorname{sign}(\tilde{f}_p) \geq -g_{mn}(\tilde{f}_p)$$
$$\geq -g_{mn}(f_p)$$
$$= (h_m - h_n)\operatorname{sign}(f_p). \tag{23}$$

Consider cycle ℓ and sum up the LHS and RHS of (22) or (23) for all p with $n_{\ell,p}^+ = 1$ to get

$$(\mathbf{n}_\ell^+)^\top \tilde{\mathbf{A}}\tilde{\mathbf{h}} > (\mathbf{n}_\ell^+)^\top \mathbf{A}\mathbf{h}. \tag{24}$$

Summing (24) over all cycles provides

$$\sum_{\ell \in \mathcal{L}} (\mathbf{n}_\ell^+)^\top \tilde{\mathbf{A}}\tilde{\mathbf{h}} > \sum_{\ell \in \mathcal{L}} (\mathbf{n}_\ell^+)^\top \mathbf{A}\mathbf{h}. \tag{25}$$

Second summand of (21). As explained earlier, if $n_{\ell,p}^+ = 1$, then $\tilde{f}_p = f_p + \alpha_\ell \geq f_p \geq 0$ so $\tilde{f}_p$ remains positive. On the other hand, if $n_{\ell,p}^- = 1$, then $\tilde{f}_p = f_p - \alpha_\ell < f_p$. In the latter case, the flow $\tilde{f}_p$ has decreased, and its sign may have been reversed to negative. Since all f_p's are positive, the flow reversals in $\tilde{f}_p$'s can be modeled as $\mathbf{A} = \mathbf{S}\tilde{\mathbf{A}}$, where matrix $\mathbf{S} := \operatorname{dg}(\operatorname{sign}(\tilde{\mathbf{f}}))$ is diagonal with the signs of $\tilde{\mathbf{f}}$ on its main diagonal. Since the vectors $\mathbf{n}_\ell$'s form a basis for $\operatorname{null}(\mathbf{A}^\top)$, it holds that $\mathbf{A}^\top \mathbf{n}_\ell = \mathbf{0}$ and so

$$(\mathbf{n}_\ell^+)^\top \mathbf{A}\mathbf{h} = (\mathbf{n}_\ell^-)^\top \mathbf{A}\mathbf{h}. \tag{26}$$

Similar properties hold for $\tilde{\mathbf{n}}_\ell := \mathbf{S}\mathbf{n}_\ell$. To see this, the vector $\tilde{\mathbf{n}}_\ell$ belongs to $\operatorname{null}(\tilde{\mathbf{A}}^\top)$ since

$$\tilde{\mathbf{A}}^\top \tilde{\mathbf{n}}_\ell = \tilde{\mathbf{A}}^\top \mathbf{S}\mathbf{n}_\ell = \mathbf{A}^\top \mathbf{n}_\ell = \mathbf{0}.$$

Therefore, we also get that

$$(\tilde{\mathbf{n}}_\ell^+)^\top \tilde{\mathbf{A}}\tilde{\mathbf{h}} = (\tilde{\mathbf{n}}_\ell^-)^\top \tilde{\mathbf{A}}\tilde{\mathbf{h}} \tag{27}$$

where $\tilde{\mathbf{n}}_\ell^+ := \max\{\tilde{\mathbf{n}}_\ell, \mathbf{0}\}$ and $\tilde{\mathbf{n}}_\ell^- := \max\{-\tilde{\mathbf{n}}_\ell, \mathbf{0}\}$.

By definition of $\tilde{\mathbf{n}}_\ell$, if $n_{\ell,p} = 1$, then $S_{p,p} = 1$ and $\tilde{n}_{\ell,p} = 1$. However, if $n_{\ell,p} = -1$, then $S_{p,p} = +1$ or $S_{p,p} = -1$ depending on the sign of $\tilde{f}_p$, and so $\tilde{n}_{\ell,p} = 1$ or $\tilde{n}_{\ell,p} = -1$. It therefore follows that

$$\mathbf{n}_\ell^+ \leq \tilde{\mathbf{n}}_\ell^+ \tag{28a}$$
$$\mathbf{n}_\ell^- \geq \tilde{\mathbf{n}}_\ell^-. \tag{28b}$$

Returning now to the ℓ-th term of the second summand in (21), we get

$$(\mathbf{n}_\ell^-)^\top \tilde{\mathbf{A}}\tilde{\mathbf{h}} \overset{a}{\geq} (\tilde{\mathbf{n}}_\ell^-)^\top \tilde{\mathbf{A}}\tilde{\mathbf{h}}$$
$$\overset{b}{=} (\tilde{\mathbf{n}}_\ell^+)^\top \tilde{\mathbf{A}}\tilde{\mathbf{h}}$$
$$\overset{c}{\geq} (\mathbf{n}_\ell^+)^\top \tilde{\mathbf{A}}\tilde{\mathbf{h}}$$
$$\overset{d}{>} (\mathbf{n}_\ell^+)^\top \mathbf{A}\mathbf{h}$$
$$\overset{e}{=} (\mathbf{n}_\ell^-)^\top \mathbf{A}\mathbf{h}. \tag{29}$$

where (a) stems from (28b); (b) from (27); (c) from (28a); (d) from (24); and (e) from (26). Summing (29) over all $\ell \in \mathcal{L}$ proves that

$$\sum_{\ell \in \mathcal{L}} (\mathbf{n}_\ell^-)^\top \tilde{\mathbf{A}}\tilde{\mathbf{h}} > \sum_{\ell \in \mathcal{L}} (\mathbf{n}_\ell^-)^\top \mathbf{A}\mathbf{h}. \tag{30}$$

Third summand of (21). The third summand sums up the pressure differences along the direction of flow for all edges not lying in any cycle. If edge $p = (m, n)$ belongs to this case (i.e., $n_p^0 = 1$), then $f_p = \tilde{f}_p$ and so as in (22) we get

$$(\tilde{h}_m - \tilde{h}_n) \operatorname{sign}(\tilde{f}_p) \geq c_{mn} \tilde{f}_p^2$$
$$= c_{mn} f_p^2$$
$$= (h_m - h_n) \operatorname{sign}(f_p).$$

Summing up the previous inequalities for all edges with $n_p^0 = 1$ yields

$$(\mathbf{n}^0)^\top \tilde{\mathbf{A}} \tilde{\mathbf{h}} \geq (\mathbf{n}^0)^\top \mathbf{A} \mathbf{h}. \tag{31}$$

Adding (24), (30), and (31) by parts gives $s(\tilde{\mathbf{h}}; \tilde{\mathbf{f}}) > s(\mathbf{h}; \mathbf{f})$. This contradicts that $(\tilde{\mathbf{f}}, \tilde{\mathbf{h}})$ is a minimizer of (W2) since $(\mathbf{f}, \mathbf{h})$ is feasible for (W2), and concludes the proof. ∎

REFERENCES

[1] H. Mala-Jetmarova, N. Sultanova, and D. Savic, "Lost in optimisation of water distribution systems? A literature review of system operation," *Environmental Modelling & Software*, vol. 93, pp. 209–254, 2017.

[2] A. Ferdowsi, A. Sanjab, W. Saad, and N. B. Mandayam, "Game theory for secure critical interdependent gas-power-water infrastructure," in *Proc. Resilience Week*, Wilmington, USA, Sep. 2017, pp. 184–190.

[3] L. A. Rossman, R. M. Clark, and W. M. Grayman, "Modeling chlorine residuals in drinking-water distribution systems," *J. of Environmental Engineering*, vol. 120, no. 4, pp. 803–820, Jul. 1994.

[4] H. D. Sherali, S. Subramanian, and G. Loganathan, "Effective relaxations and partitioning schemes for solving water distribution network design problems to global optimality," *J. of Global Optimization*, vol. 19, no. 1, pp. 1–26, Jan. 2001.

[5] C. D'Ambrosio, A. Lodi, S. Wiese, and C. Bragalli, "Mathematical programming techniques in water network optimization," *European J. of Operational Research*, vol. 243, no. 3, pp. 774 – 788, Jun. 2015.

[6] D. Denig-Chakroff, "Reducing electricity used for water production: Questions state commissions should ask regulated utilities," *Water Research and Policy*, Jun. 2008.

[7] J. E. Van-Zyl, D. A. Savic, and G. A. Walters, "Operational optimization of water distribution systems using a hybrid genetic algorithm," *J. of Water Resources Planning and Management*, vol. 130, no. 2, pp. 160–170, 2004.

[8] D. Fooladivanda and J. A. Taylor, "Energy-optimal pump scheduling and water flow," *IEEE Trans. Control of Network Systems*, vol. 5, no. 3, pp. 1016–1026, Sep. 2018.

[9] M. K. Singh and V. Kekatos, "Optimal scheduling of water distribution systems," *IEEE Trans. Control of Network Systems*, 2018, (submitted). [Online]. Available: http://arxiv.org/abs/1806.07988

[10] E. Todini and L. A. Rossman, "Unified framework for deriving simultaneous equation algorithms for water distribution networks," *J. of Hydraulic Engineering*, vol. 139, no. 5, pp. 511–526, May 2013.

[11] L. Jun and Y. Guoping, "Iterative methodology of pressure-dependent demand based on EPANET for pressure-deficient water distribution analysis," *J. of Water Resources Planning and Management*, vol. 139, no. 1, pp. 34–44, Jan. 2013.

[12] L. A. Rossman, "EPANET 2 user's manual," 2000.

[13] E. Todini, "On the convergence properties of the different pipe network algorithms," in *Water Distribution Systems Analysis Symp.*, Reston, VA, Mar. 2006, pp. 1–16.

[14] M. Bazrafshan, N. Gatsis, M. Giacomoni, and A. Taha, "A fixed-point iteration for steady-state analysis of water distribution networks," in *Proc. IEEE Global Conf. on Signal and Information Process.*, Anaheim, CA, Nov. 2018.

[15] S. Elhay, A. R. Simpson, J. Deuerlein, B. Alexander, and W. H. A. Schilders, "Reformulated co-tree flows method competitive with the global gradient algorithm for solving water distribution system equations," *Journal of Water Resources Planning and Management*, vol. 140, no. 12, p. 04014040, Dec. 2014.

[16] F. Alvarruiz, F. Martinez-Alzamora, and A. M. Vidal, "Improving the efficiency of the loop method for the simulation of water distribution systems," *J. of Water Resources Planning and Management*, vol. 141, no. 10, pp. 04015019.1–04015019.10, Oct. 2015.

[17] S. Elhay, J. Deuerlein, O. Piller, and A. R. Simpson, "Graph partitioning in the analysis of pressure dependent water distribution systems," *J. of Water Resources Planning and Management*, vol. 144, no. 4, p. 04018011, Apr. 2018.

[18] H. Zhang, X. Cheng, T. Huang, H. Cong, and J. Xu, "Hydraulic analysis of water distribution systems based on fixed point iteration method," *Water Resources Management*, vol. 31, no. 5, pp. 1605–1618, Mar. 2017.

[19] C. Estrada, C. Gonzlez, R. Aliod, and J. Pao, "Improved pressurized pipe network hydraulic solver for applications in irrigation systems," *J. of Irrigation and Drainage Engineering*, vol. 135, no. 4, pp. 421–430, Aug. 2009.

[20] D. Verleye and E.-H. Aghezzaf, "Optimising production and distribution operations in large water supply networks: A piecewise linear optimisation approach," *Intl. J. of Production Research*, vol. 51, no. 23-24, pp. 7170–7189, 2013.

[21] D. Cohen, U. Shamir, and G. Sinai, "Optimal operation of multi-quality water supply systems-II: The Q-H model," *Engineering Optimization*, vol. 32, no. 6, pp. 687–719, 2000.

[22] B. Ulanicki, J. Kahler, and B. Coulbeck, "Modeling the efficiency and power characteristics of a pump group," *J. of Water Resources Planning and Management*, vol. 134, no. 1, pp. 88–93, 2008.

[23] C. Godsil and G. Royle, *Algebraic Graph Theory*. New York, NY: Springer, 2001.

[24] M. K. Singh and V. Kekatos, "Natural gas flow equations: Uniqueness and an MI-SOCP solver," 2018, submitted June 2018. [Online]. Available: https://arxiv.org/abs/1809.09025

[25] D. De Wolf and Y. Smeers, "The gas transmission problem solved by an extension of the simplex algorithm," *Management Science*, vol. 46, no. 11, pp. 1454–1465, Nov. 2000.

[26] S. Boyd and L. Vandenberghe, *Convex Optimization*. New York, NY: Cambridge University Press, 2004.

[27] D. Fooladivanda and J. A. Taylor, "Optimal pump scheduling and water flow in water distribution networks," in *Proc. IEEE Conf. on Decision and Control*, Osaka, Japan, Dec. 2015, pp. 5265–5271.

[28] P. D. Aylett, "The energy-integral criterion of transient stability limits of power systems," *Proc. of the IEE – Part C: Monographs*, vol. 105, no. 8, pp. 527–536, Sep. 1958.

[29] A. R. Bergen and D. J. Hill, "A structure preserving model for power system stability analysis," *IEEE Trans. Power App. Syst.*, vol. 100, no. 1, pp. 25–35, Jan. 1981.

[30] K. Dvijotham, E. Mallada, and J. W. Simpson-Porco, "High-voltage solution in radial power networks: Existence, properties, and equivalent algorithms," *IEEE Control Systems Lett.*, vol. 1, no. 2, pp. 322–327, Oct. 2017.

[31] S. Taheri and V. Kekatos, "Power flow solvers for direct current networks," 2018, submitted October 2018. [Online]. Available: https://arxiv.org/abs/1807.03936

[32] R. Z. Ríos-Mercado, S. Wu, L. R. Scott, and E. A. Boyd, "A reduction technique for natural gas transmission network optimization problems," *Annals of Operations Research*, vol. 117, no. 1, pp. 217–234, Nov. 2002.

[33] A. Atamtürk and V. Narayanan, "Conic mixed-integer rounding cuts," *Mathematical Programming*, vol. 122, no. 1, pp. 1–20, Mar. 2010.

[34] J. Lofberg, "YALMIP: a toolbox for modeling and optimization in MATLAB," in *IEEE Intl. Conf. on Robotics and Automation*, New Orleans, LA, Sep. 2004, pp. 284–289.

[35] IBM Corp., "IBM ILOG CPLEX Optimization Studio CPLEX User's Manual," 2017. [Online]. Available: http://www.ibm.com